

Formation of Hydroxyapatite Coating by Mechanical Alloying Method

A. Hannora^{1*}, A. Mamaeva², N. Mofa³, S. Aknazarov^{1,3}, Z. Mansurov^{1,3}

¹al-Farabi Kazakh National University, 050038, Almaty, Kazakhstan

²Institute of Physics and Technology, 050032, Almaty, Kazakhstan

³Institute of combustion problems, 050012, Almaty, Kazakhstan

Abstract

Hydroxyapatite [$\text{Ca}_{10}(\text{PO}_4)_6(\text{OH})_2 - \text{HA}$] material has been clinically applied in many areas of dentistry and orthopaedics. Presented work describes the effect of mechanical alloying treatment, as a non-conventional solid-state process, on the microstructure of hydroxylapatite powder and Ti-alloy substrate. The relationship between the crystallinity, crystallite size and strain of the HA with milling factors was investigated. Milled HA powders and Ti-substrate were characterized by X-Ray Diffraction (XRD) and/or scanning probe microscope (SPM) using atomic force microscopy (AFM). Increasing the ratio of the weight of the ball to the powder ($W_b:W_p$) ratio and milling time accelerates the broadening and intensity reduction of XRD peaks. There was no evidence that milling time up to 2 hrs or $W_b:W_p$ can change chemical composition of the HA. Decomposition of HA phase or secondary phases such as α and/or β -tri-calcium phosphate (α , β – TCP), and calcium oxide (CaO) was not observed throughout the milling process. The average grain size and the internal strain are calculated from the XRD by Scherrer's formula and Hall–Williamson method. The Ti doped HA samples shows a notable broadening and intensity reduction comparing with HA powders before and after milling.

Introduction

Calcium phosphate-based ceramic-coated titanium and titanium alloys have become one of the most promising implant materials for orthopaedic and dental applications this is due to their favourable biocompatibility and mechanical properties. Among the entire calcium phosphate family, the most interesting material is perhaps hydroxyapatite, due to its stability in contact with body fluids. Also, the use of nanocrystalline HA as a reactant offers a novel route to the production of brushite cements [1,2]. This mineral, along with fluorapatite ($\text{Ca}_5(\text{PO}_4)_3\text{F}$), monetite (CaHPO_4), tricalcium phosphate ($\text{Ca}_3(\text{PO}_4)_2$), tetracalcium phosphate ($\text{Ca}_4(\text{PO}_4)_2$), and octacalcium phosphate ($\text{Ca}_8\text{H}_2(\text{PO}_4)_6.5\text{H}_2\text{O}$), belongs to a family of minerals known as apatites. These materials demonstrate similar structures (hexagonal system, space group, $\text{P6}_3/\text{m}$), and possess the structural formula

$X_3Y_2(\text{TO}_4)Z$. In nature, apatite compositions include X and $Y = \text{Ca, Sr, Ba, Re, Pb, U, or Mn}$ (rarely Na, K, Y, Cu); $T = \text{P, As, V, Si, S, or CO}_3$; and $Z = \text{F, Cl, OH, or O}$. In medicine, apatites of interest possess $X = Y = \text{Ca}$, $T = \text{P}$, and $Z = \text{F or OH}$. In the case of hydroxyapatite, $T = \text{P}$ and $Z = \text{OH}$. Hydroxyapatite is similar to the biological apatites that provide strength to the skeleton and act as a storehouse for calcium, phosphorus, sodium, and magnesium [3].

The methods of coating deposition are numerous and varied, and usually involve liquid phase processing, or gas/vapour state. It is hard to name a technique for depositing a coating in the solid state, without the use of solvent or an intermediate liquid. A recently developed technique, mechanical alloying, seems to be appropriate for this purpose. The basis of new method rests with the investigations of the process of metal oxide reduction in various reducing mediums under impulsive mechanical activation conditions. It is well known that mechanical activation initiates and accelerates chemical interactions in the solid phase. Using this method, pure metallic coatings on dissimilar substrates can be ob-

*corresponding author. E-mail: ahannora@yahoo.com

tained, and alloy coatings of different compositions be produced [4,5]. Mechanical alloying/milling is a solid-state powder processing technique involving cold-welding and fracturing of powder particles. The constituent powder particles are repeatedly fractured and cold welded, so that powder particles with very fine structure can be obtained after milling [6].

The objective of this first study was to examine the effects of the following three variables on the structure stability properties of HA: the weight of the ball to the powder ratio, milling time, and Ti-additives to improve the bond strength of HA. Also the effect of milling time on Ti-substrate had to be studied. Another aim of the present work was to study the effect of the best milling parameters (time of milling and ball to powder weight ratio) for coating hydroxyapatite on Ti-substrate by mechanical alloying method as a new method for coating.

Materials and Methods

Commercial hydroxyapatite powder (Sigma-Aldrich), Ti-powder (Wako, 99.5%, 250 μm) and 10 \times 8 \times 2 mm Ti-alloy substrates were milled for various time. Also, the HA powder was milled with different weight to powder ratios. The powders and/or Ti-substrate with steel balls (5 mm) were placed into the vibration chamber vibrated by mechano-reactor. HA powders were put into cylindrical hardened tool steel vial (20 cm^3). The milling process was carried out in static air without process control agent. The chamber was just O-ring sealed in order to prevent contamination from the atmosphere. After mechanical treatment, the titanium samples were cleaned in an ultrasonic alcohol for 60 second at 35 $^\circ\text{C}$.

XRD patterns data through the process of milling are essential to follow and understanding mechanism of microstructure transformation. XRD was performed using DRON-6 system. Diffraction measurements were performed using Cu K_α radiation (wavelength $\lambda = 0.15406 \text{ nm}$) with a nickel filter at 25 kV and 25 mA. The diffractometer was operated within rang of $20 < 2\theta < 60$ with step-time = 3 seconds and step-size = 0.02 degree. Diffraction signal intensity throughout the scan was monitored and processed with PDWin software. Standard database for powder diffraction were used for comparing results. The surface topography of the titanium samples was examined with scanning probe microscope (SPM) using atomic force microscopy (AFM).

Results and Discussion

In order to improve the mechanical properties of hydroxyapatite, the properties of the powder have to be studied by controlling important parameters such as particle size and shape, particle distribution and agglomeration [7]. The function of HA in all of its applications is largely determined by its morphology, stoichiometry, crystallinity, and crystal size distribution. For example, nanosize HA powders are sintering reactive, and the highly densified and refined microstructure. Derived from a nano-sized, HA powder can lead to a significant improvement in mechanical properties of sintered HA, and therefore widens its applications as load-bearing implants [8]. The milling process is affected by several factors that are playing very important roles in the fabrication of homogeneous materials. It is well known that the properties of the milled powders of the final product, such as the particle size distribution, the degree of disorder, or amorphization, and the final stoichiometry, depend on the milling conditions and, as such, the more complete the control and monitoring of the milling conditions, the better end product is obtained [6].

Milling media-to-powder weight ratio is one of the most important factors which affecting the final product. Figure 1 shows the XRD of the mechanical milled HA powders processed for various weight of the ball to the powder ($W_b:W_p$) ratio for one hour. With increasing $W_b:W_p$ ratio the XRD patterns show a notable broadening and intensity reduction. Based on their results [6,9], the rate of amorphization depends strongly on the kinetic energy of the ball mill charge and this depends on the number of opportunities for the powder particles to be reacted and inter-diffused. Increasing the ratio accelerates the rate of amorphization, which is explained by the increase in the kinetic energy of the ball mill charge per unit mass of powders. The volume fraction of the amorphous phase in the mechanically alloyed ball milled powders increases with increasing $W_b:W_p$ ratio, up to 1:40. It is noted that further increasing this weight ratio leads to the re-crystallization of HA powder and this could be related to the high kinetic energy of the ball mill charge which transformed into heat. Decomposition of HA or secondary phases were not observed throughout the milling process.

The measurement of crystallite size and lattice strain in the mechanically milled powders is very important since the phase constitution and transformation characteristics appear to be critically dependent

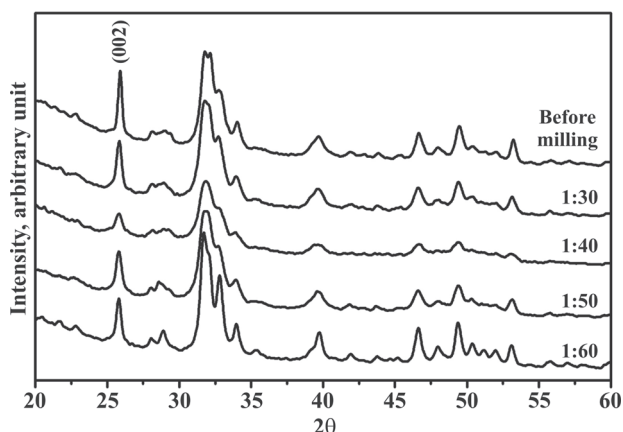


Fig. 1. XRD patterns of hydroxyapatite powder milled one hour for various $W_b:W_p$ ratio.

on them. The Scherrer's formula estimate the size (d) of very small crystals from the measured width (B) of their diffraction curves as [10].

$$d = \frac{\lambda}{B \cos \theta} \quad (1)$$

The width B is usually measured, in radians, at an intensity equal to half the maximum intensity, and this measure of width is termed the full-width at half the maximum (FWHM). The B parameter was corrected using the following equation:

$$B = \sqrt{B_{Exp}^2 - B_{Inst}^2}$$

where B_{Inst} corresponds to instrumental width and B_{Exp} corresponds to experimental FWHM obtained for each sample. While the X-ray peak broadening due to small crystallite size is inversely proportional to $\cos \theta$, that due to lattice strain (ϵ) is proportional to $\tan \theta$:

$$B = k \cdot \epsilon \cdot \tan \theta \quad (2)$$

Where, k is a constant that depends on the definition of a micro-strain. The average grain size and the internal strain are calculated from the XRD by the Hall-Williamson method [11]. The Hall-Williamson equation is expressed as:

$$B \cos \theta = \frac{0.9 \lambda}{d} + 2 \epsilon \sin \theta \quad (3)$$

FWHM was evaluated using a Pseudo Voigt fit with double K_α peak separation.

For measuring the crystallite size and lattice strain in the mechanically milled powders, the most distinction reflection in the XRD patterns was chosen, the single peak near 25.8 degree. And according to $P6_3/m$ space group of HA, this peak corresponds to $hkl = 002$. Using equation (1) and (2), the calculated

mean crystallite size of the milled HA samples decreases during the milling time while the micro-strain increases up to 40 min. The excessive cold working of the powder during mechanical milling leads to the formation of high density of defects that could hold responsible for the observed high strain in the sample. With increasing $W_b:W_p$ ratios more than 1:40, the mean crystallite size increases while micro-strain decreases and saturated after 1:60. This could be related to the high kinetic energy of the ball mill charge which transformed into heat. Drastic fragmentation of the crystallites is achieved at low $W_b:W_p$ ratios of the milling process with a large increase on the internal strain. Upon further milling, the strain still increases in the lattice and reaches values that provoke, at 1:40 ratio. After that the strain decreases and the crystal size slightly increases. Not only the grain size decreased with $W_b:W_p$ ratios but the area under the XRD peaks also. The area under the diffracted peaks could be taken as an indicator for the degree of crystallinity where the crystallinity reduced with $W_b:W_p$ ratios Fig. 2b. When the ratio increases more than 1:40, the crystallinity increases again and saturated after 1:60.

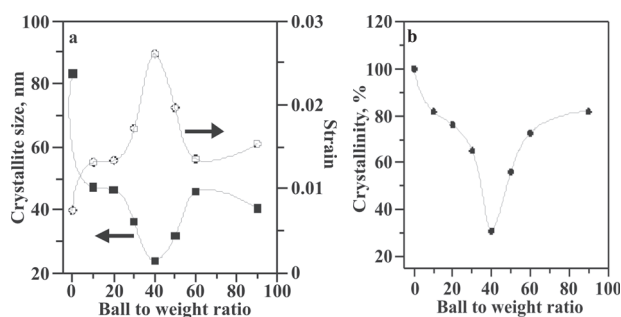


Fig. 2. a – Variation of crystallite size (nm) ■ and strain ○ with ball to weight ratios. b – Crystallinity % variation with ball to weight ratio.

Another important factor affecting the mechanically alloyed end product is the milling time. Figure 3 shows the XRD of the mechanical milled HA powders with weight of the ball to the powder ratio 1:40, processed for various milling time. Using higher weight ratios could produce high concentration of iron contamination which is introduced to the milled powders during the milling process. With increasing milling time, the XRD patterns also shows a notable broadening and intensity reduction. It is also generally observed from XRD patterns that, the powder remains crystalline and no change tendency was

manifested. On the other hand, after one hour of milling there is no more broadening and intensity reduction. There was no evidence that milling time up to 2 hrs can change chemical composition of the HA.

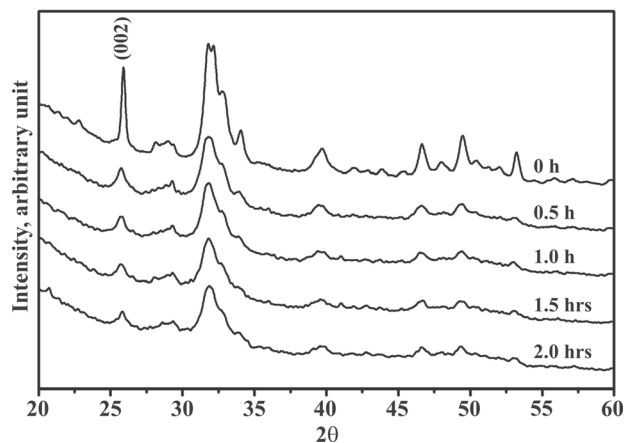


Fig. 3. XRD patterns of hydroxyapatite powder milled for various time.

As shown in Figure 4a, up to 40 minute, the obtained mean crystallite size of the milled HA samples decreases during the milling time while the micro-strain increases. With increasing milling time, the variation becomes relatively stable. The excessive cold working of the powder during mechanical milling leads to the formation of high density of defects that could hold responsible for the observed high strain in the sample. Also the crystallinity reduced with milling time Fig. 4b.

In addition to synthesizing stable (equilibrium) solid solutions, it has also been possible to synthesize metastable (non-equilibrium) supersaturated solid solutions by MA starting from blended elemental powders in several binary and higher order systems. The solid solubility limit is expected to increase

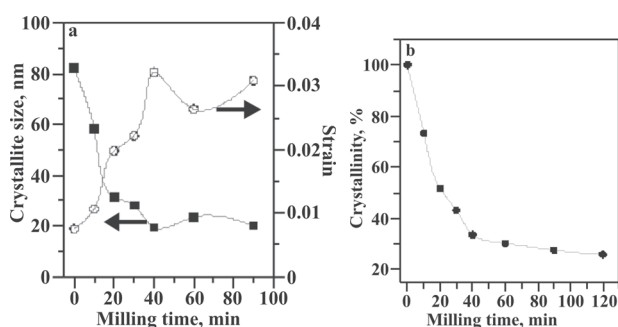


Fig. 4. a – Variation of crystallite size ■ and strain ○ with milling time b – Normalized fraction of the crystalline phase as a function of milling time.

with milling time as diffusion progresses and reach a (super)saturation level, beyond which no further extension of solid solubility occurs. This saturation value has been listed as the solid solubility level achieved by MA. Solid solubility levels have been generally determined from changes in the lattice parameter values calculated from shifts in peak positions in the X-ray diffraction patterns. Very frequently, the absence of second phase reactions in the X-ray diffraction patterns has been inferred as the absence of a second phase, and hence the formation of a homogeneous solid solution [6]. Figure 5a and b shows the XRD patterns of the pure HA powder before and after milling for 1 h, while Fig. 5c, d and e shows the XRD patterns for 5 wt.% Ti-doped HA powder milled for various time. Significant changes were detected in the XRD patterns when HA mechanochemically treated. The Ti doped sample shows a notable broadening and intensity reduction comparing with HA powders before and after milling. Due to the mechanical deformation introduced into the powder and Ti solubility, the particle and crystallite could be refined and the lattice strain increases more than the pure HA. It is reported that, Ti incorporation into the apatite structure caused lattice shrinkage and the grain sizes of substituted HA were smaller than those of pure HA. Increasing the amount of the Ti ions in HA caused the decomposition of HA [12].

As seen in Figure 5, the (002) reflections of the as treated HA powders containing Ti^{4+} shifted to lower angles this could indicate that Ca^{2+} cations were substituted by Ti^{4+} . The homogeneous distribution of Ti particles in the HA formed by MA could improve the bonding strength between coating and substrate. With increases milling time of the Ti-doped HA the broadening increases and intensity faster reduced.

Optimization of the surface structure of materials is of great concern at the present time since most failures occur on the surface (fatigue, fretting corrosion, corrosion, wear, etc.). As a result, improving the surface properties would greatly enhance the overall behaviour of materials. The importance of the surface structure and the attractive properties afforded by nanostructured materials have led to the development of a new concept called surface nanocrystallization [13]. It is widely recognized that titanium displays poor wear resistance and that its fatigue performance depends to a large extent on its surface properties. The newly developed MA process is therefore of considerable technological importance since it provides the possibility of dramatically improving

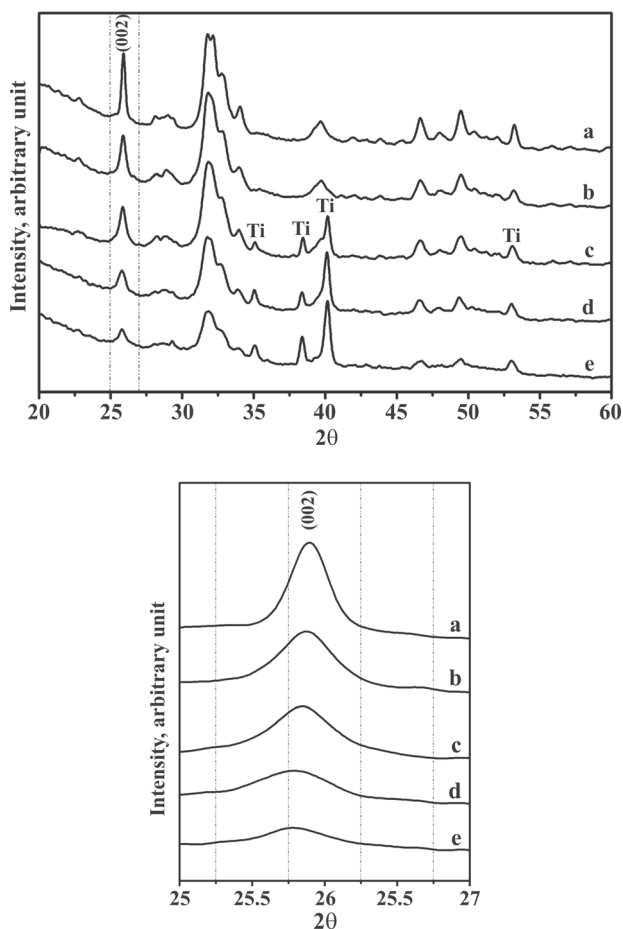


Fig. 5. XRD patterns of hydroxyapatite powder (a) before milling, (b) after 1 h milling and (c, d, e) 5 wt.% Ti-doped milled for 1, 1.5, 2 hrs respectively.

the surface properties of titanium. As a result, extended applications which demand high levels of reliable performance can be anticipated in surgery and medicine as well as in the aerospace, automotive, chemical plant, power generation and other major industries [5]. Figure 6 shows the XRD of the mechanical milled titanium samples with weight of the ball to the powder ratio 1:40, processed for various milling time. With increasing milling time, the XRD patterns also shows a notable broadening and intensity reduction up to one hour. Through the milling process the titanium sample loss parts of it weight as a result of impaction, Fig. 7.

The average grain size and the internal strain of the milled titanium samples were calculated from the XRD by the Hall-Williamson method, eq. (3). Figure 8 shows the Hall-Williamson plot of one hour milled titanium sample. Using the least-squares fitting equations, the mean crystallite sizes and strains were evaluated. After 30 min. of milling the crystallite size and

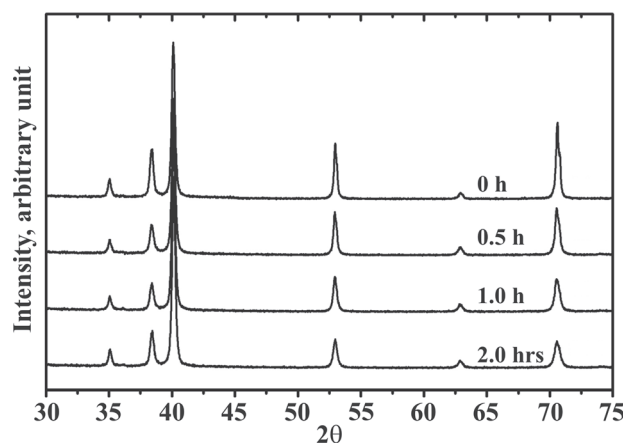


Fig. 6. XRD patterns of titanium substrate milled for various time.

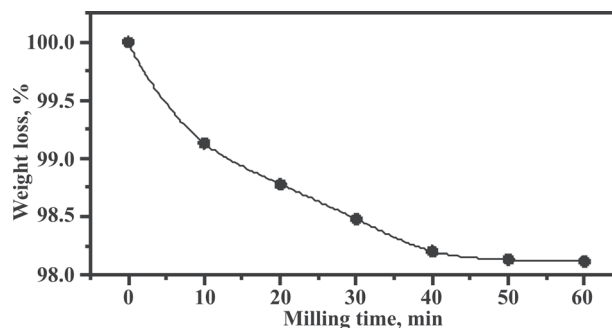


Fig. 7. Titanium sample weight loss with milling time.

micro-strain was 120.4 nm and 0.00263, while after 60 min. it was 84.7 nm and 0.00198 respectively.

Figure 9 presents a typical surface topography of titanium substrate obtained by AFM under conditions identical to those of HA powder. The particle size of the titanium sample before treatment was 0.3-0.5 mm while the sample treated for one hour it was less than 80 nm. It is concluded that, as the strain and strain rate increase, the following changes occur in the microstructure of titanium during surface mechanical attrition treatment (1) the onset of twins and the intersection of twin systems, (2) the formation of low angle disoriented lamellae displaying a high density of dislocations, (3) the subdivision of microbands into blocks and the resulting formation of polygonal sub-

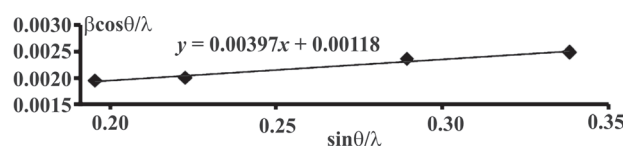


Fig. 8. Hall-Williamson plot of one hour milled titanium sample (θ in radians).

micronic grains and (4) The further breakdown of submicronic polygonal grains into nanograins [13]. As seen in Figure 7, as the strain increases the scale of the microstructure reduce very rapidly, this could be due to the further formation of twins. Also, additional strain accommodation is achieved by successive grain subdivision.

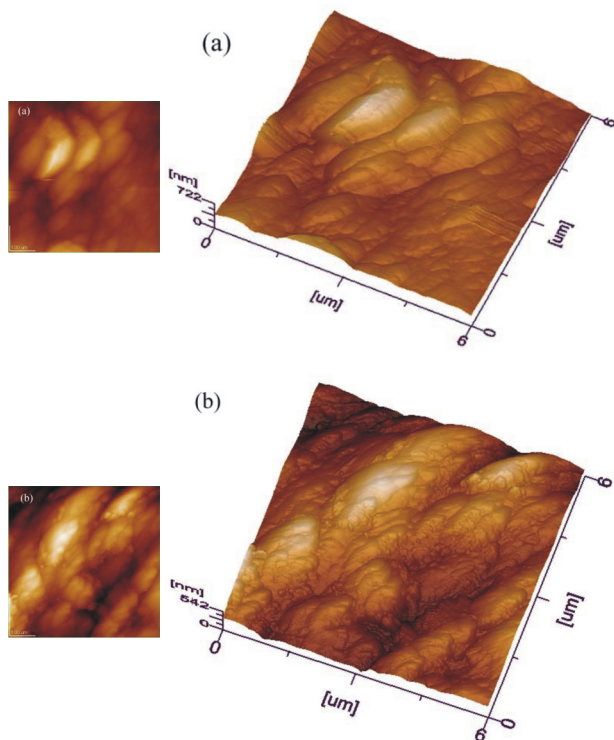


Fig. 9. Two and three dimension topography of titanium substrate (a) before milling, (b) after one hour of milling.

However, the interface between HA and a metallic implant has been another matter of concern in terms of the mechanical properties and biocompatibility of the implant. In order for the HA coating to be effective and reliable, it must be strongly bonded to the metallic surface. For this reason, chemical bonding derived from the reaction/diffusion at the HA-metal interface could develop a highly reliable interface in response to this requirement. While the presence of reaction/diffusion bonding at the interface may increase the bond strength between HA and the metal, since this new interface material has a different composition from HA or the metal, it may cause toxic reactions in the body [14]. Adding Ti particles as second phase to HA aims to improving the bonding strength between coating and substrate. It is conclude that [15], the bond strength of the composite coating has been improved by the addition of Ti and increases

with an increase in Ti content. The strengthening mechanism of the co-deposited HA/Ti composite coatings should relate to the dispersion strengthening by homogeneous distribution of Ti particles in the HA. Other factor, the coefficient of thermal expansion (CTE) of HA was $15 \times 10^{-6} \text{ K}^{-1}$ and that of Ti was $8.6 \times 10^{-6} \text{ K}^{-1}$. It is also likely that the bonding strength of HA/Ti coating can be improved through a mechanism in which the CTE mismatch between the HA/Ti coating and the Ti substrate is reduced.

XRD patterns of deposited HA and 5 wt.% Ti-doped HA are presented in Fig. 10. The changes in the XRD patterns give an indication of the influence of milling process on the structure stability of the samples. X-ray peaks of the formed phase were matched to the ICDD (JCPDS) standard, α -tricalcium phosphate (09-0348), β -tricalcium phosphate (03-0690) and titanium oxide (29-1361). XRD patterns of the HA and 5 wt.% Ti-doped HA shows the Ti substrate and HA peaks. The Ti doped samples shows a notable broadening and intensity reduction comparing with pure HA after milling. The wide peaks of the deposited materials should be due to very small crystallite size.

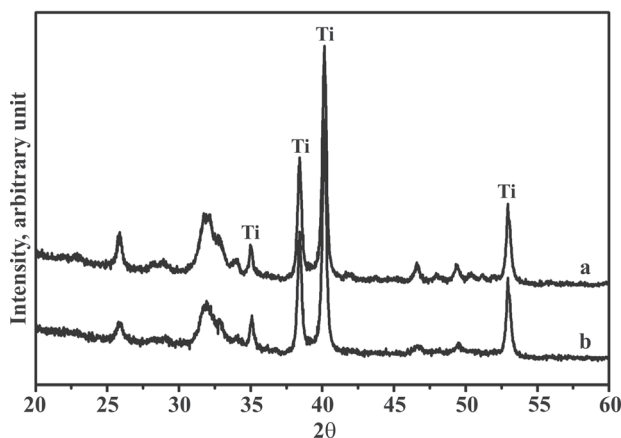


Fig. 10. XRD patterns of (a) HA and (b) 5 wt.% Ti added HA coating on titanium substrate.

Backscattered electron images of the coated titanium alloy substrate surface were shown in Fig. 11. After one hour of milling, the substrate was partially covered with powder. The inhomogeneous distribution over the entire coated sample could be due to powder particles repeatedly fractured and cold welded on the substrate. Relatively larger covered area of the Ti-doped HA coating with respect to pure HA was seen. This could be due to Ti addition which improves the bond strength of HA.

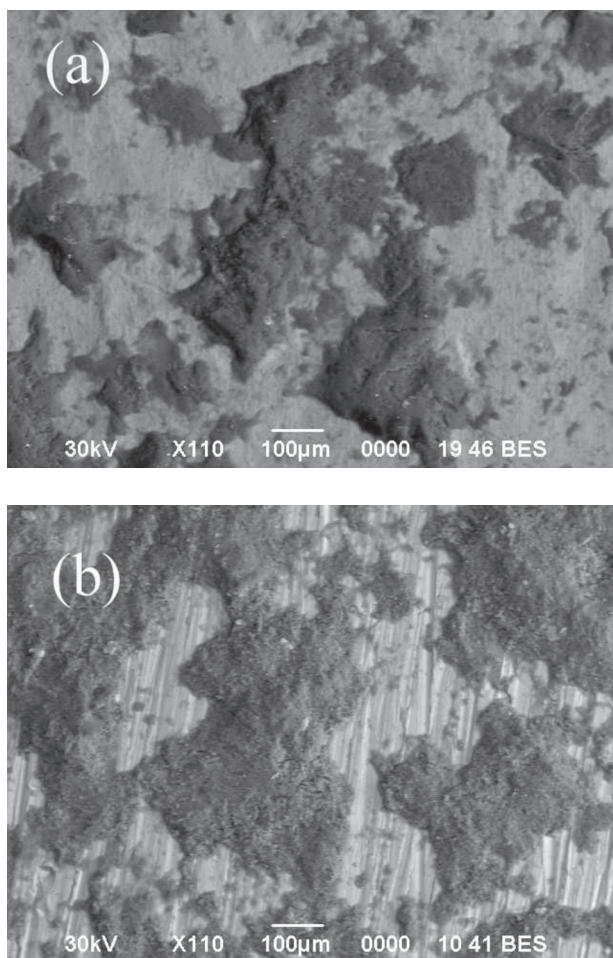


Fig. 11. Backscattered electron images of the as-synthesized (a) pure HA and (b) 5 wt.% Ti-doped HA coating after one hour of milling.

Conclusions

From the structural point of view, and independently of the milling times or weight of the ball to the powder ratio, the structure of HA powder have not any phase transition or decomposition. A nanostructured surface, less than 80 nm was produced on Ti substrate by ball milling. HA and 5 wt.% Ti-doped HA deposited on Ti substrate at room temperature by mechanical alloying technique. From the structural point of view the as-synthesized sample has not any phase transition or decomposition. The Ti doped sample shows a notable broadening and intensity re-

duction comparing with HA powders before and after milling. Ti incorporation into the apatite structure caused lattice shrinkage.

Reference

1. Wang C.K., Chern Lin J.H., Ju C.P., Ong H.C., Chang R.P.H., *Biomaterials* 18:1331, (1997).
2. Chean P. and Khor K.A., *Biomaterials*, 17:537, (1996).
3. White T., Ferraris C., Kim J. and Madhavi S., *Rev. in Min. & Geochem.* 57:307, (2005).
4. Romankov S., Sha W., Kaloshkin S.D., Kaevitser K., *Surface & Coatings Technology* 201:3235 (2006).
5. Torosyan A., Tuck J., Korsunsky A., Bagdasaryan S.A., *Materials Science Forum*, 386-388: 251 (2002).
6. Suryanarayana C., *Prog. In Mater. Sci.* 46:1 (2001).
7. Shih W.J., Wang J.W., Wang M.C., Hon M.H., *Mater. Sci. & Eng. C* 26:1434 (2006).
8. Li H., Zhu M.Y., Li L.H., *J. Mater. Sci.* 43:384 (2008).
9. El-Eskandarany, M.S., Aoki, K., Itoh, H. and Suzuki, K., *J. Less-Common Met.* 169, 235 (1991).
10. Pecharsky V.K., Zavalij P.Y. *Fundamentals of powder Diffraction and structural characterization of materials*, Library of Congress Cataloging-in-Publication Data, p. 172. (2005).
11. Sastry K.Y., Froyen L., Vleugels J., Van der Biest O., Schattevoy R., Hennicke J., *Rev. Adv. Mater. Sci.* 8:34 (2004).
12. Ribeiroa C. Gibsond I., Barbosa M. *Biomaterials.*, 27:1749 (2006).
13. Zhu K.Y., Vassel A., Brisset F., Lu K., Lu J., *Acta Materialia* 52:4100(2004).
14. Ergun C., Doremus R., *Turkish J. Eng. Env. Sci.* 27:423 (2003).
15. Xiao X.F., Liu R.F., Zheng Y.Z., *Materials Letters*, 59:1660 (2005).

Received 12 October 2008.